Journal of Artificial Organs (2018) 21:238–246
https://doi.org/10.1007/s10047-017-1014-1

ORIGINAL ARTICLE

Artificial Skin, Muscle, Bone / Joint, Neuron

Rapid prototyping prosthetic hand acting by a low-cost shape-memory-alloy actuator

Enrique Soriano-Heras[1] · Fernando Blaya-Haro[2] · Carlos Molino[2] · José María de Agustín del Burgo[2]

Received: 29 August 2016 / Accepted: 26 December 2017 / Published online: 8 January 2018

Abstract
The purpose of this article is to develop a new concept of modular and operative prosthetic hand based on rapid prototyping and a novel shape-memory-alloy (SMA) actuator, thus minimizing the manufacturing costs. An underactuated mechanism was needed for the design of the prosthesis to use only one input source. Taking into account the state of the art, an underactuated mechanism prosthetic hand was chosen so as to implement the modifications required for including the external SMA actuator. A modular design of a new prosthesis was developed which incorporated a novel SMA actuator for the index finger movement. The primary objective of the prosthesis is achieved, obtaining a modular and functional low-cost prosthesis based on additive manufacturing executed by a novel SMA actuator. The external SMA actuator provides a modular system which allows implementing it in different systems. This paper combines rapid prototyping and a novel SMA actuator to develop a new concept of modular and operative low-cost prosthetic hand.

Keywords Rapid prototyping · Shape-memory-alloy · Low-cost prosthesis · Underactuated mechanism

List of symbols

$\vec{q}$	Coordinates' vector
$\vec{\Phi}$	Constraint equations' system
x_i	Horizontal coordinate
y_i	Vertical coordinate
θ, α_1	Angular coordinate
L_{ij}	Bar length
λ_i	Proportionality constant
$\dot{\theta}$	Angular speed
$\ddot{\theta}$	Angular acceleration

Introduction

The evolution of prosthetics is a long and storied history, from its primitive beginnings to its sophisticated present, to the exciting visions of the future. As in the development of any other field, some ideas and inventions have worked and been expanded upon, while others have fallen by the wayside or become obsolete, such as the use of iron in prosthesis [1].

Nowadays, there is a wide range of hand prosthesis to approach all the different requirements of handicapped people. How do modern prosthetic limbs compare to those of historical times? One major difference is the presence of newer materials, such as advanced plastics and carbon-fibre composites. These materials can make a prosthetic limb lighter, stronger, and more realistic. Electronic technologies make today's advanced prosthetics more controllable, even capable of automatically adapting their function during certain tasks, such as gripping or walking [2].

It is possible to find many commercial prosthesis that can be bought by paying a large amount of money; however, the development of new fabrication techniques like rapid prototyping machines allows reducing the price and time of producing specific final products [3] for each patient. Due to the decrease in the cost of fused deposition modelling (FDM), the most widespread of the low-cost rapid prototyping technologies nowadays, the development of hand designs in FDM has increased [4–6].

Moreover, new materials have also been developed that can be used to produce a movement as the case of shape-memory-alloy (SMA), which eliminates the need to use motors to produce a movement. An SMA "remembers"

✉ Enrique Soriano-Heras
esoriano@ing.uc3m.es

1 Universidad Carlos III de Madrid, Leganés, Madrid, Spain

2 ETSIDI, Universidad Politécnica de Madrid, Madrid, Spain

its original shape, and after being deformed, it returns to its pre-formed shape when heated. This material is a light-weight, solid-state alternative to conventional actuators such as hydraulic, pneumatic, and motor-based systems [7–10].

In recent years, different ways of acting on prosthesis have been developed. Traditionally, there have been used linear actuators, stepper motors, and servomotors. This is the case of Openbionics, which developed a bionic hand that can be produced with a 3D printer which uses linear actuators [5]. Some other devices use servomotors and transform the motion using different configurations of gears [11].

However, the weight and dimensions associated with suitable DC motors are not always compatible with the geometric restrictions of a prosthetic hand, thus reducing the available degrees of freedom and ultimately rendering the prosthesis uncomfortable for the end-user. Because of these limitations, the search is on-going to find a more appropriate actuation solution that is lightweight, strong, and cheap. The development of active materials, such as electroactive polymers or SMAs, that are operationally similar to the human muscle, have encouraged the development of hands [7]. The SMA describes the process of a material changing shape or remembering a particular shape at a specific temperature. The shape-memory effect is due to the phase transformation from the austenite (parent) phase to martensite (product) phase and vice versa. These transformations take place because of changes in temperature or stress, or else a combination of both. To activate the SMA material, an energy input is required [12, 13].

There are different ways to provide energy through.

- Electric currents circulating in the SMA. These currents increase the material temperature.
- External heating. Through convection, radiation, and conduction.

Materials which can only exhibit the shape change or memory effect once are known as one-way SMAs. However, some alloys can be trained to show a two-way effect in which they remember two shapes, one below and one above the memory temperature. Nitinol is biocompatible; that is, it can be used in the body without an adverse reaction, so it has found a number of medical uses [14–16].

There are different options to implement these materials. In most cases, the actuation mechanism is comparable to the biological muscle—they contract, thus producing actuation forces [9, 10].

These muscle-like actuators present a high power to weight ratio, thus enabling the development of compact, lightweight prosthetic devices without too much compromising of its power capabilities and eliminating the forced-tradeoff between dexterity and anthropomorphic size, weight, and appearance [8].

These methods implement the SMA material for an internal actuation of hand prosthesis, but any of them propose an external actuation method with a low-cost SMA actuator, which allows obtaining a modular system.

The purpose of this article is to combine these two techniques to develop a new concept of operative prosthetic hand based on rapid prototyping and SMA actuator, minimizing the metallic pieces to reduce manufacturing costs.

Materials and methods

Design of the SMA actuator

The actuator is composed by a light 3D printed base, a stainless steel beam, a nitinol wire (for technical data see [17]), hooked by two stainless steel parts, two 3D-printed pieces and a bolt and nut, see Fig. 1a. A nylon wire in the free end

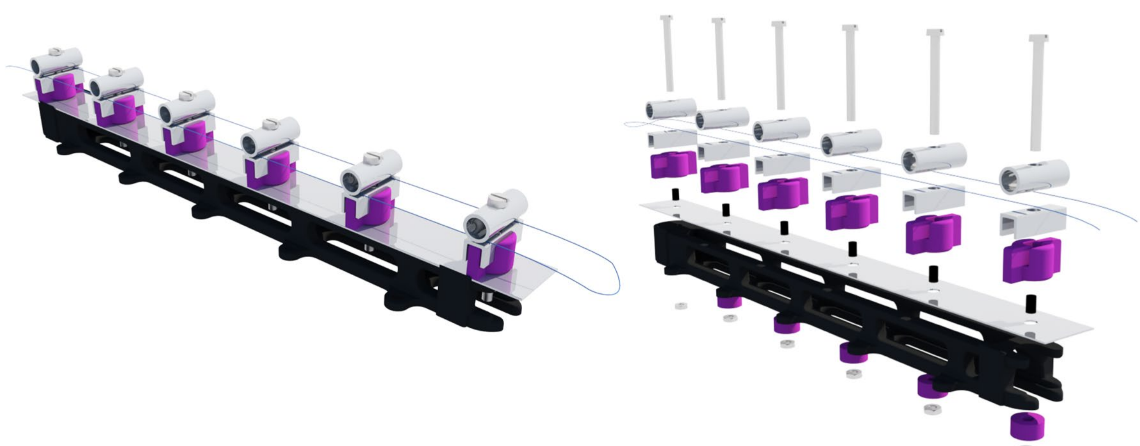

(a) (b)

Fig. 1 SMA actuator design and an exploded view detailing all parts of the beam was attached to transfer the lineal displacement to the mechanism.

The beam is fixed by six points to the nitinol wire and the beam itself is fixed to the plastic base from an end side. When the SMA wire heats, by the transmission of an electric current through the wire, it shrinks and forces the beam to flex, thus making the free end of the beam to rise from the base. This electrical current (3A 3V approximately) is transmitted from the power source to two of the six attachment points. Depending on the selection of these points, it is possible to obtain 15 different positions of the actuator. The amount of flex depends on the shrinkage of the SMA wire that is the selected electrical input points, obtaining the maximum flexion value through the extreme points due to the five nitinol section contract at the same time. Because of that, the experimental tests were carried out with this configuration of the input terminals. The flexion movement is transformed in lineal actuation using a nylon wire to transfer the movement. The nitinol wire used met the mechanical requirements for this application, although other diameter size could be chosen.

The two stainless steel pieces, that trap the nitinol wire, are supported by 3D-printed parts to insulate the electrical transmission to the beam, and also a section of a heat shrinkable tube has been added in the region of the bolt which adjoins with the beam, for the same reason (see Fig. 1b). The 3D-printed part below (purple piece) separates the nut from the steel beam.

Design of hand prosthetic

As it was said in "Introduction", the development of hand prosthesis in FDM is usual nowadays. Among all these projects, the "Hackberry" [6, 18] presents an underactuated finger mechanism, which allows controlling the complete mechanism movement with only one actuator. Because of that, the development of this prosthesis was based on Hackberry design, performing all the modifications needed to obtain a modular and functional hand prosthetic acted by an SMA actuator. It was decided to implement the SMA actuator just for the movement of the index finger, considering that the actuation of the remaining fingers could be easily made in the future.

Index finger

The index finger of the prosthesis was designed in five parts to adapt the model to two phalanges (see Fig. 2a). The ultimate black piece acts like the intermediate and distal phalanges joined, and the remaining parts act like the proximal phalange. The yellow parts were divided into two pieces, so that they could be printed easily. The links between the bars and with the palmar region structure were obtained with five rotary joints. The motion is transmitted to the input crank of the actuated finger by means of a gear.

The design provides two different types of movement to the index finger thanks to the brake bar (see Fig. 2b) located inside the yellow part bellow. When this part is not blocked by the grasped object, the torsion spring, placed concentrically to the rotary axis that joints the yellow part above and the ultimate black piece (see Fig. 2b), forces all the parts to act like a solid rigid body rotating around the attachment point to the bench (case 1 of the analytical model, see Fig. 3a), but if the brake bar is locked by the reaction force generated by the grasped object, the finger will act like a four bar linkage (case 2 of the analytical model, see Fig. 3b). In this first investigation, only case 1 had been experimented and case 2 has been propose as a possible open work, in "Conclusions".

Thumb

The purpose of the thumb is to catch the object when the finger moves down. It was designed in two possible

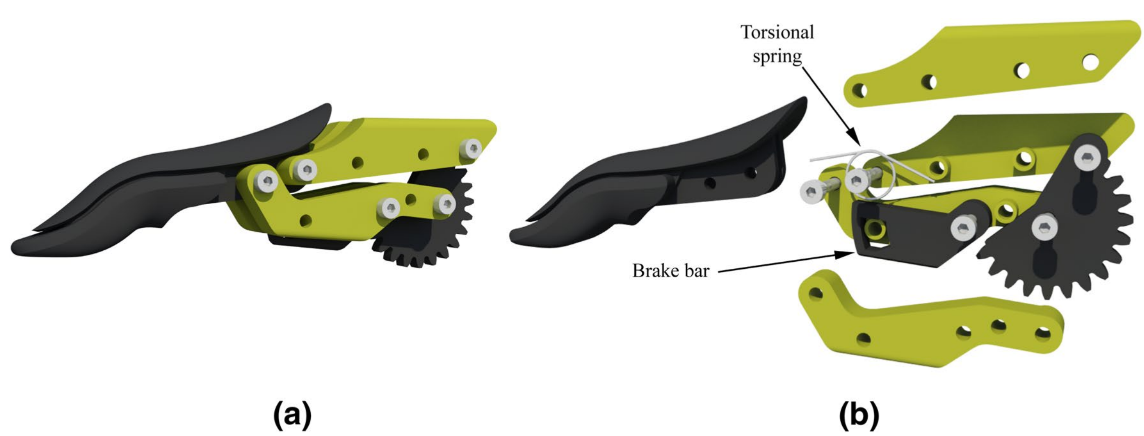

Fig. 2 Finger hand design and an exploded view of the internal components of the finger

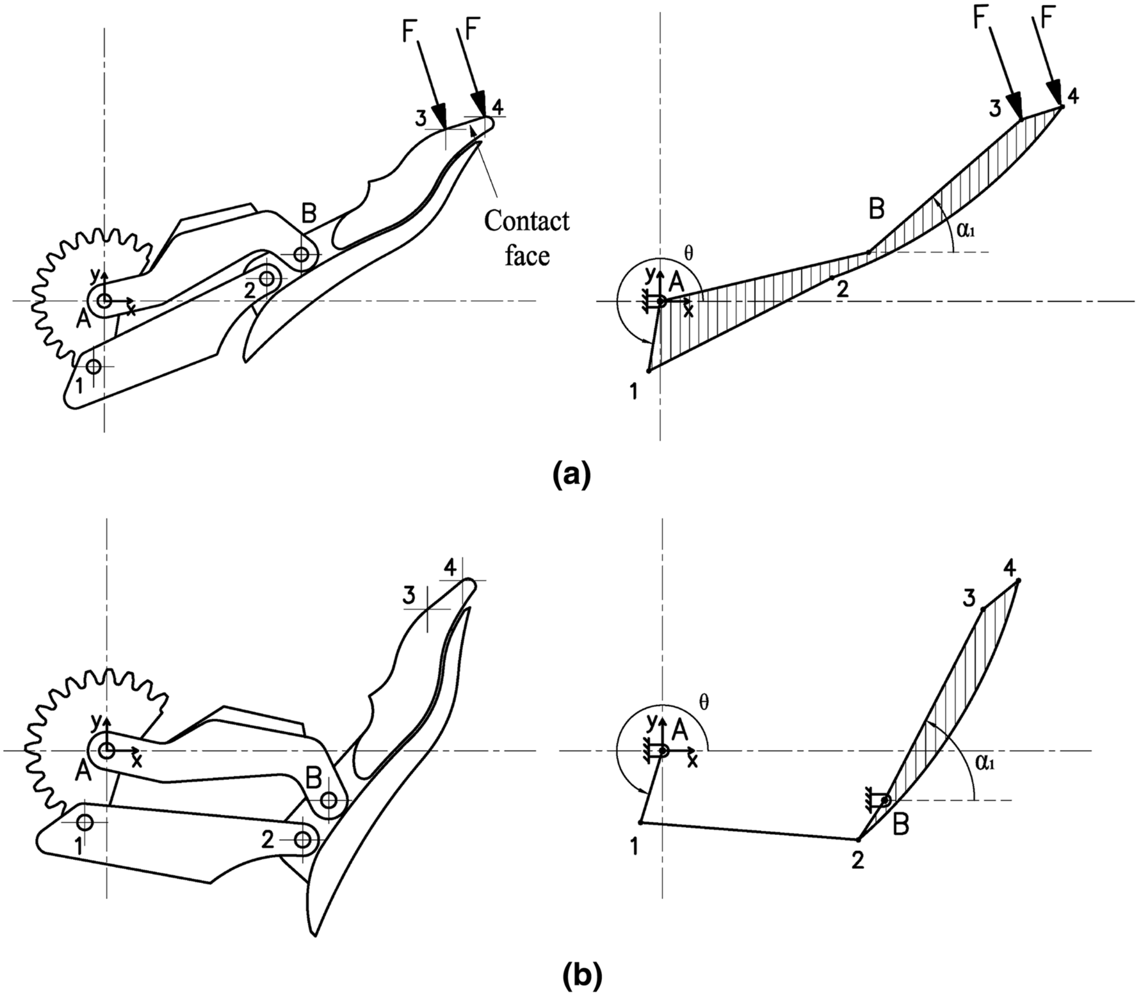

Fig. 3 Analytical model sketches of cases 1 and 2, showing the utilized coordinates in both cases and the supposed forces for the dynamic model of case 1

configurations held by a fastener. The first one is the functional position and it is aligned with the index finger. The second position available is merely aesthetic to look like a real relaxed open hand. The user can decide between both arrangements by removing the fastener and placing the thumb to the wanted position.

The thumb was composed by two phalanges (the ultimate black piece acts like the distal phalange and the yellow acts like the proximal phalange) joined to the palmar region by a support part (black piece). Both phalanges are linked by a rotary joint with a torsional spring concentrically located inside. The rotating movement was added just for the reason of avoiding a possible damage in the prosthesis at the grasping moment, so it was limited to a reduced rank. The spring has the mission to maintain the distal phalange in its upper position and to hold the grasped object.

Palmar region structure

The coupler between the SMA actuator to the hand prosthesis must transform the linear displacement provided by the actuator to a rotary motion of the input crank of the finger. This transformation was carried out by a system composed by two pulleys that guide the nylon wire linked to the actuator. One of the pulleys was joined to the input gear thus obtaining a single printed piece; see Fig. 4a. The nylon wire was fit to the pulley gear and a torsion spring was added (placed concentrically to the rotary axis) to keep the tension along the cable when the actuator goes down.

To improve the functionality of the hand, three radial bearings were added: two of them for the gear pulley, so that the whole axis rotates synchronously (this execution permits to attach rotary encoder wheel for obtaining measurements of angular position) and one for the single pulley, see

Fig. 4 Design of the movement transmission system detailing internal parts and fully assembled hand design

Fig. 4a. Although the index finger is the functional one, the remaining fingers were added to the prosthesis to improve the aesthetic of the hand, as shown in Fig. 4b.

Analytical model of the index finger mechanism

As the hand prosthesis finger has two cases of mechanism motion, the analytical model to obtain the kinematic and dynamic results was made separately for each one.

Both study case models were developed in natural coordinates and solved by the Newton–Raphson method and the virtual work theorem for the kinematic and dynamic analysis severally. The natural coordinate method can be programmed easily in MATLAB and provides a high precision result thus avoiding possible uncertainty points.

In both cases, the degree of freedom (DOF) is one; so the angle (θ), speed ($\dot{\theta}$), and acceleration ($\ddot{\theta}$) of the input crank were introduced as the known freedom degree in the calculation of position, speed and acceleration of all the variables.

The kinematic analysis obtains the results of position, speed and acceleration of the mechanism variables in all positions of the movement range. Conversely, in the dynamic analysis of the prosthetic hand finger, the reaction forces appear at the precise moment of the contact between the finger and the grabbed object, because of that, the dynamic analysis was developed for the last point of the kinematic analysis (which had been supposed for the contact moment). This analysis is an inverse dynamic problem because the computed forces/moments are based on the kinematic analysis.

Case 1: solid rigid crank

For the first case, the coordinates' vector ($\vec{q}$) was defined with the ten natural coordinates of the mechanism and two angular relative coordinates, see Fig. 3a. This vector represents the position of all the coordinates as a function of the known freedom degree (θ):

$$\vec{q} = \left\{\theta, \alpha_{1,} x_1, y_1, x_2, y_2, x_3, y_3, x_4, y_4, x_{\mathrm{B}}, y_{\mathrm{B}}\right\}. \tag{1}$$

With Eq. 1, the constraint equations' system ($\vec{\Phi}$) has been obtained (shown in Eq. 2) that completely defines the mechanism. It is composed by nine rigid solid equations (which define the mechanism dimensions) and four angular relative coordinate equations (which relate the relative coordinates with the natural coordinates):

$$\vec{\Phi}(\vec{q}) = \left\{\begin{array}{c} {x_1}^2 + {y_1}^2 - {L_{1\mathrm{A}}}^2 \\ \left(x_2 - x_1\right)^2 + \left(y_2 - y_1\right)^2 - {L_{21}}^2 \\ {x_2}^2 + {y_2}^2 - {L_{2\mathrm{A}}}^2 \\ \left(x_3\right) - \lambda_1\left(x_1\right) - \lambda_2\left(x_2\right) \\ \left(y_3\right) - \lambda_1\left(y_1\right) - \lambda_2\left(y_2\right) \\ \left(x_4\right) - \lambda_3\left(x_1\right) - \lambda_4\left(x_2\right) \\ \left(y_4\right) - \lambda_3\left(y_1\right) - \lambda_4\left(y_2\right) \\ \left(x_{\mathrm{B}}\right) - \lambda_5\left(x_1\right) - \lambda_6\left(x_2\right) \\ \left(y_{\mathrm{B}}\right) - \lambda_5\left(y_1\right) - \lambda_6\left(y_2\right) \\ x_1 - L_{1\mathrm{A}} \cdot \cos\theta \\ y_1 - L_{1\mathrm{A}} \cdot \mathrm{sen}\theta \\ \left(x_3 - x_{\mathrm{B}}\right) - L_{3\mathrm{B}} \cdot \cos\alpha_1 \\ \left(y_3 - y_{\mathrm{B}}\right) - L_{3\mathrm{B}} \cdot \mathrm{sen}\alpha_1 \end{array}\right\} = 0. \tag{2}$$

It is used the Newton–Raphson method for solving this system of equations. Therefore, the position results ($\vec{q}$) are obtained. The values of speed ($\dot{\vec{q}}$) and acceleration ($\ddot{\vec{q}}$) are procured from the first and the second derivative of Eq. (2) with respect to time respectively.

As it was mention at "Analytical model of the index finger mechanism", the virtual work theorem in natural coordinates is utilized for the dynamic analysis in the last point of the kinematic analysis. The Lagrange multiplayers are implemented for the resolution of this method.

The mechanical advantage (MA) measures the relation between the input torque and the output punctual forces. Accordingly, a point force ($F = 1$N) at each endpoint of the finger (points 3 and 4) in the normal direction of the contact face (see Fig. 3a) were supposed to get the values of the MA in these locations.

Case 2: four bar linkage

For the second case, the coordinates' vector ($\vec{q}$) was defined with the eight natural coordinates of the mechanism and two angular relative coordinates, see Fig. 3b:

$$\vec{q} = \left\{\theta, \alpha_{1,} x_1, y_1, x_2, y_2, x_3, y_3, x_4, y_4\right\}. \tag{3}$$

As in the previous case, with Eq. 3, the constraint equations' system ($\vec{\Phi}$), shown in Eq. 4, has been obtained by seven rigid solid equations and four angular relative coordinate equations:

$$\vec{\Phi}(\vec{q}) = \left\{ \begin{array}{c} {x_1}^2 + {y_1}^2 - {L_{1A}}^2 \\ \left(x_2 - x_1\right)^2 + \left(y_2 - y_1\right)^2 - {L_{21}}^2 \\ \left(x_B - x_2\right)^2 + \left(y_B - y_2\right)^2 - {L_{B2}}^2 \\ \left(x_3 - x_B\right)^2 + \left(y_3 - y_B\right)^2 - {L_{3B}}^2 \\ \left(x_3 - x_2\right)^2 + \left(y_3 - y_2\right)^2 - {L_{32}}^2 \\ \left(x_4 - x_2\right) - \lambda_1\left(x_B - x_2\right) - \lambda_2\left(x_3 - x_2\right) \\ \left(y_4 - y_2\right) - \lambda_1\left(y_B - y_2\right) - \lambda_2\left(y_3 - y_2\right) \\ x_1 - L_{1A} \cdot \cos\theta \\ y_1 - L_{1A} \cdot \mathrm{sen}\theta \\ \left(x_3 - x_B\right) - L_{3B} \cdot \cos\alpha_1 \\ \left(y_3 - y_B\right) - L_{3B} \cdot \mathrm{sen}\alpha_1 \end{array} \right\} = 0. \tag{4}$$

As it is mentioned in "Index finger", only case 1 has been resolved in this first investigation.

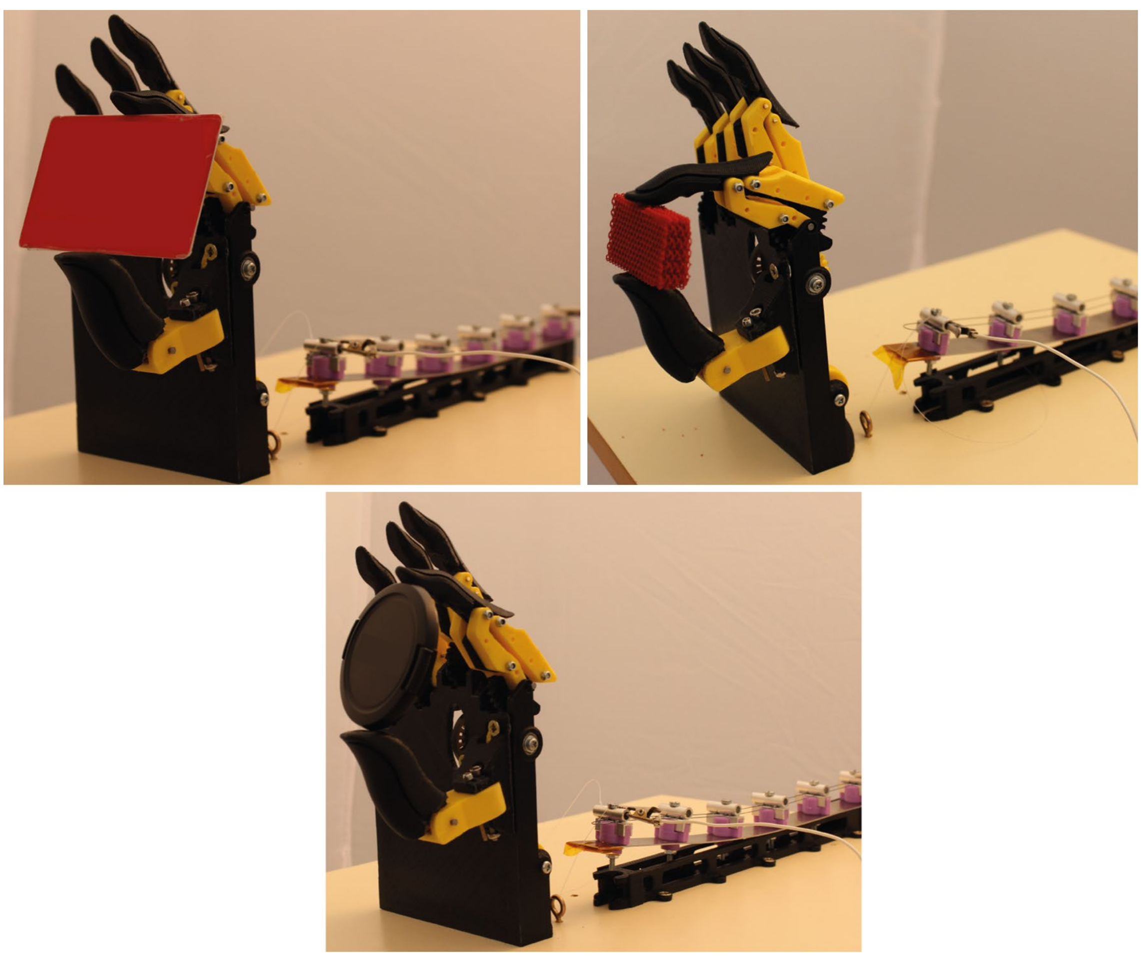

Fig. 5 Grasping of different objects using the presented prosthesis

Experimental tests

Obtaining input data for case 1

To introduce real values into the analytical model, the range of the position values of the input crank, as a function of time, was obtained with an optical position rotary encoder sensor. The graduated wheel was fixed to the gear axis, so the ensemble could rotate synchronously. Thanks to this electronic device, the input variables were easily stored in an excel file, where they can be imported in the MATLAB software so as to get the kinematic and dynamic results.

Grasping test

The presented prosthesis was able to grasp several light objects of different shapes, as shown in Fig. 5.

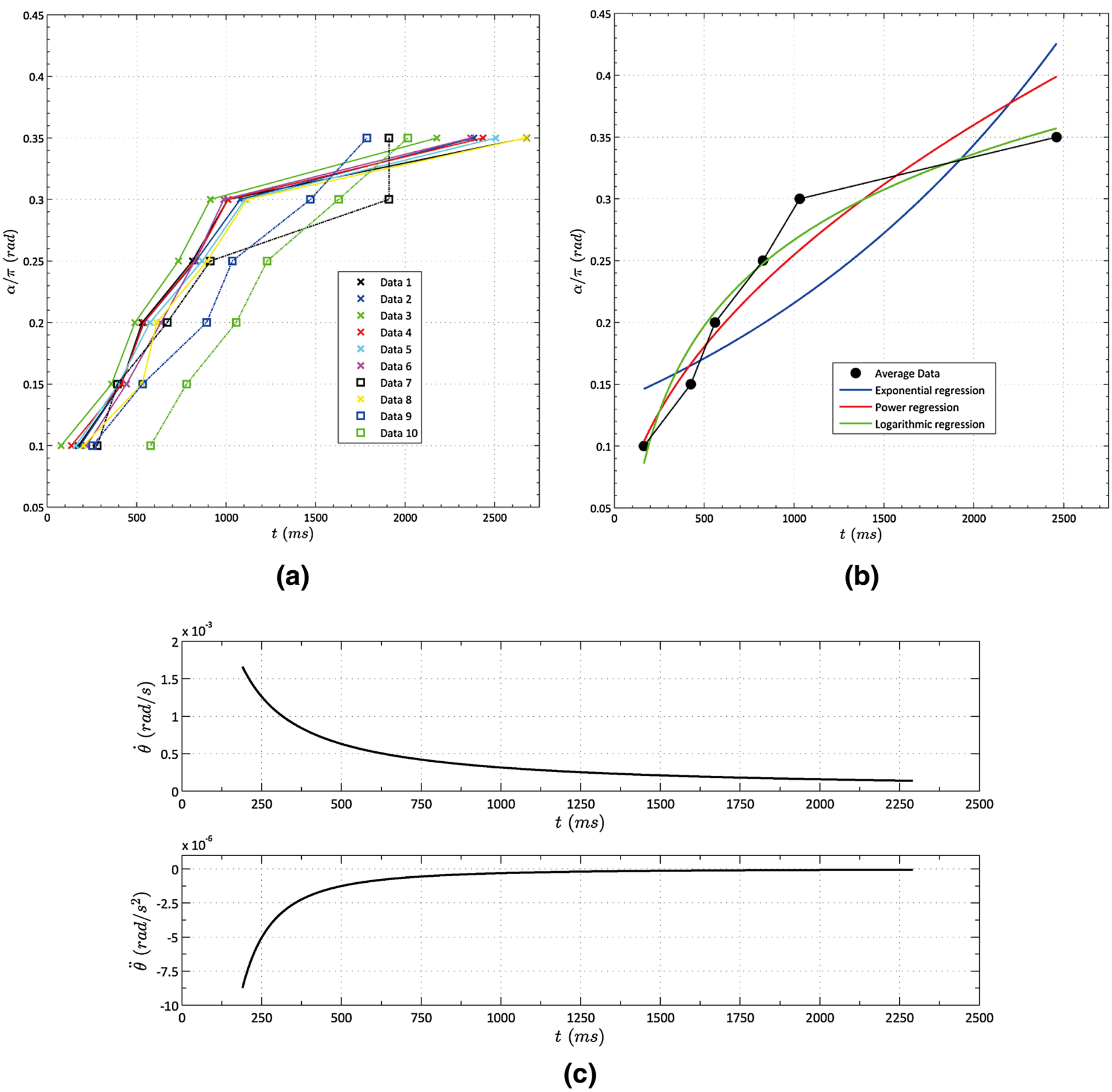

Fig. 6 Graphics of experimental measure data point sets of angular position as a function of time

Results

The kinematic values of the input crank were experimentally obtained to introduce the most approximate data set to the real ones. In the Fig. 6a, the ten measure data sets that had been obtained are shown. Three of these data sets (7, 9, and 10) were discarded to improve the average data accuracy. These average points were fitted to three different types of regression curves to approach the experimental points to a mathematical formula, see Fig. 6b.

The best adjustment curve was the logarithmic regression, green line of Fig. 6b. Accordingly, it has been used as the position of the known freedom degree. With the first and second derivatives with respect to time of this curve, the values of speed and acceleration were obtained:

$$\begin{cases} \Delta\theta = 0.3155 \cdot \mathrm{Ln}(t) - 1.3416 \\ \Delta\dot{\theta} = 0.3155 \cdot \frac{1}{t} \\ \Delta\ddot{\theta} = -0.3155 \cdot \frac{1}{t^2} \end{cases} . \quad (5)$$

By applying the reference system utilized in "Case 1: solid rigid crank" to Eq. 5, the graphics of the known freedom degree were obtained, see Fig. 6c. The most significant part of the finger is the end side (points 3 and 4), where the contact with the object is produced; therefore, the graphic results of speed and acceleration of both points were obtained (see Fig. 7).

To obtain the mechanical advantage of the index finger, it is necessary to obtain the relation between the input and the output forces. Therefore, the values of this ratio in both end-points were procured: 0.4744 in point 3 and 0.5256 in point 4.

Discussions

The kinematic graphic results show that speed and acceleration of finger end-points start at the maximum values and approach to zero as the time increases (see Fig. 7). Although it seems to be counter-productive, a low value of the speed at the grasping moment decreases the possibility of producing damage to the hand, considering that the complete prosthetic is fabricated with plastic, so it has not high mechanical performance.

The mechanical advantage of the prosthetic finger indicates that the input force applied needs to be two times the output force. Although this value is not too efficient, this is not very significant in the validation of the prosthesis.

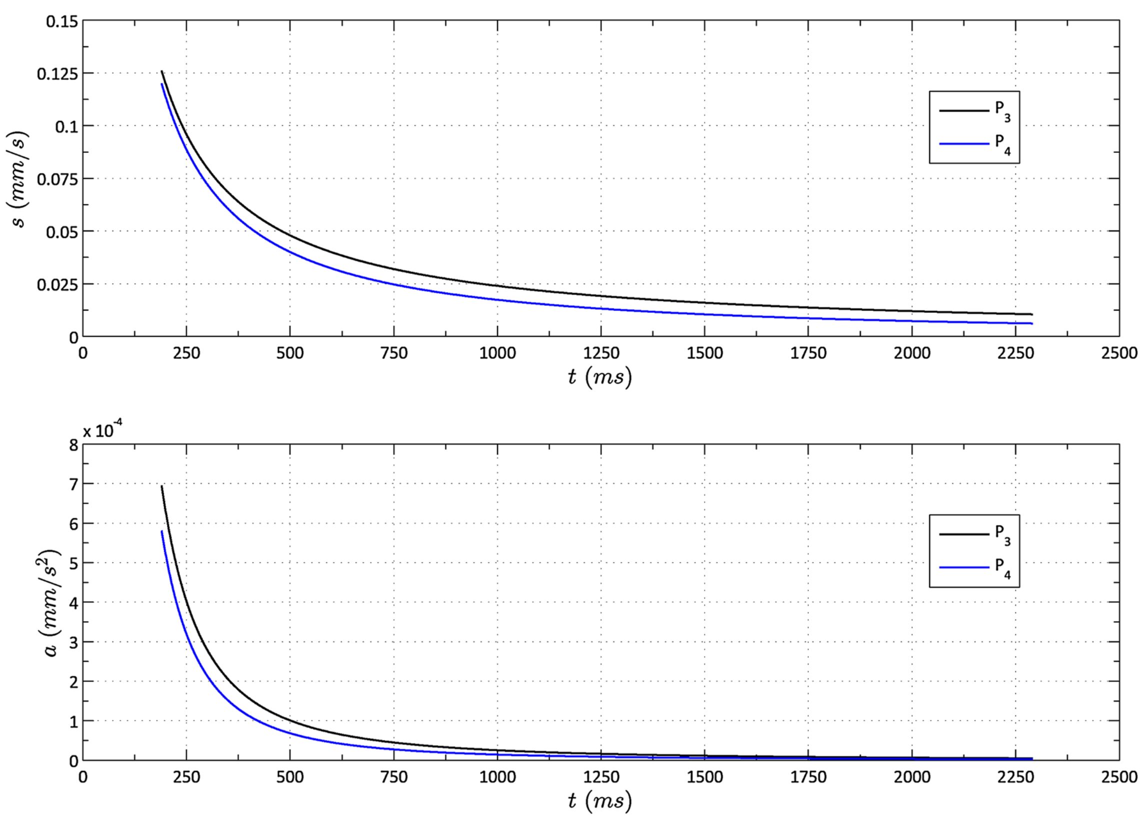

Fig. 7 Speed and acceleration graphic results of the end-points 3 and 4 of case 1

The results of the grasping test connote that the pressure at the fingertip has a low value now that only lightweight objects could be grasped.

Conclusions

The prototype of the prosthesis is made by additive manufacturing technology, attaining the minimum number of metallic pieces used, which enhances an appreciable reduction on the final price of the product. The low-cost SMA actuator allows, when the electric field passes through the nitinol wire, moving the index finger, thanks to its underactuated mechanism design, with only one input source.

Therefore, the primary objective of this paper is achieved, thus obtaining a low-cost operative prosthetic hand based on additive manufacturing, applying a novel shape-memory-alloy actuator for the movement of the underactuated index finger movement.

Besides, there are some open work lines to improve the hand. It could be possible to actuate the remaining fingers, to obtain a complete analysis of the case 2 of the finger mechanism or to enhance the motion transformation mechanism to obtain a higher value of the pressure at the fingertip. Another interesting enhancement would be to connect the SMA actuator to a sensory receptor to respond to a stimulus of the brain. Furthermore, it could be workable to test the different positions of the actuator, by selecting the input current points, as well as implement an electronic control device to select these points automatically.

References

1. Zuo KJ, Olson JL. The evolution of functional hand replacement: from iron prostheses to hand transplantation. Plast Surg. 2014;22(1):44–51.
2. Perry I. How prosthetic limbs work, (online) HowStuffWorks. 2008. http://science.howstuffworks.com/prosthetic-limb2.htm. Accessed 11 May 2016.
3. Hophinson N, Dickens P. Rapid prototyping for direct manufacture. Rapid Prototyp J. 2001;7(4):197–202.
4. Enabling the Future. Enabling the future. 2016. http://enablingthefuture.org/. Accessed 12 March 2016.
5. Open Bionics. Home. 2016. http://www.openbionics.com/. Accessed 12 March 2016.
6. Exiii-hackberry.com. HACKberry Open source community. 2016. http://exiii-hackberry.com/. Accessed 13 March 2016.
7. Kaplanoglu E. Design of shape memory alloy-based and tendon-driven actuated fingers towards a hybrid anthropomorphic prosthetic hand. Int J Adv Robotic Syst. 2012. https://doi.org/10.5772/51276.
8. Simone F, York A, Seelecke S. Design and fabrication of a three-finger prosthetic hand using SMA muscle wires. In: International society for optics and photonics. Bioinspiration, biomimetics, and bioreplication, vol 9429. 2015; p. 94290T. https://doi.org/10.1117/12.2084524.
9. Yee CA, Kasim M, Koch T, Dumitrescu R, Yussof H, Jaafar R, Jaffar A, Aqilah A, Mun K. Hybrid-actuated finger prosthesis with tactile sensing. Int J Adv Robotic Syst. 2013;10:1.
10. She Y, Li C, Cleary J, Su H. Design and fabrication of a soft robotic hand with embedded actuators and sensors. J Mech Robot. 2015;7(2):021007.
11. Tlegenov Y, Telegenov K, Shintemirov A. 2014. An open-source 3D printed underactuated robotic gripper, mechatronic and embedded systems and applications (MESA), 2014 IEEE/ASME 10th international conference, pp. 1–6, IEEE.
12. Bundhoo E, Haslam B, Birch E, Park J. A shape memory alloy-based tendon driven actuation system for biomimetic artificial fingers. Part I design and evaluation. Robotica. 2008;27(1):131–146.
13. Andrianesis K, Tzes A, Nikolakopoulos G, Koveos Y. Experimental study of a shape memory alloy actuation system for a novel prosthetic hand. In: Cismasiu Corneliu, editor. Shape memory alloys. London: INTECH, Open Access Publisher; 2010.
14. Otsuka K, Kakeshita T. Science and technology of shape-memory alloys: new developments. MRS Bull. 2002;27(02):91–100.
15. Hodgson DE, Wu MH, Biermann RJ. Shape memory alloys. Metals handbook. Vol 2. Ohio: ASM International; 1990.
16. Huang W. 1998. Shape memory alloys and their application to actuators for deployable structures. PhD Thesis, University of Cambridge, Peterhouse.
17. Dynalloy.com. Flexinol® actuator wire technical and design data. 2016. http://www.dynalloy.com/tech_data_wire.php. Accessed 23 April 2016.
18. Smith M. Handie prosthetic uses 3D printing and smartphones for much cheaper bionic hands (video). 2013. https://www.engadget.com/2013/11/03/handie-prosthetic-cheaper-smartphone-3d-printing/. Accessed 13 March 2016.